The International Journal of Advanced Manufacturing Technology (2022) 118:3315–3330
https://doi.org/10.1007/s00170-021-08138-4

ORIGINAL ARTICLE

Study on magnetic abrasive finishing process of AlSi10Mg alloy curved surface formed by selective laser melting

Yuntao Cui[1] · Guixiang Zhang[1] · Tonglei Cui[1] · Peixin Zhu[1] · Jiajing Du[1] · Ning Liu[1] · Haoxin Chen[1]

Received: 19 July 2021 / Accepted: 27 September 2021 / Published online: 13 October 2021

Abstract
In this paper, AlSi10Mg alloy powder is selected as the forming powder of Selective laser melting technology, and the AlSi10Mg alloy SLM curved surface sample is constructed by setting the internal and external layering parameters. In view of the relatively rough surface roughness of SLM technology molded parts, this paper selects the magnetic finishing technology with higher flexibility characteristics to perform surface finishing and finishing on the formed curved surface samples. Explore the feasibility of magnetic finishing technology on the finishing of SLM shaped curved parts, and test and analyze the surface roughness, surface hardness and hydrophobicity of the finishing permanent magnet tools and the curved surface samples before and after finishing. Finally, it was found that the use of a 75° trapezoidal slotted permanent magnet finishing tool to absorb spherical Al2O3 magnetic abrasives for flexible finishing of AlSi10Mg alloy SLM shaped curved surface samples can achieve better finishing results. In this paper, the orthogonal experiment method is used to optimize the finishing experiment. It is found that the finishing parameters of the spindle speed is 1800 r/min, the feed rate is 5 mm/min, the gap is 2 mm, and the abrasive consumption is 7 g to form the AlSi10Mg alloy SLM. The surface roughness Ra = 0.279 μm can be obtained by magnetic finishing of the curved sample, and the surface morphology of the sample has been greatly improved. At the same time, it is found that the magnetic finishing technology improves the surface roughness of the AlSi10Mg alloy SLM forming surface sample, while it does not change the surface hardness of the sample, but it can significantly improve the hydrophobicity of the sample surface.

Keywords Magnetic abrasive finishing (MAF) · Selective laser melting (SLM) · AlSi10Mg alloy curved surface · 75° trapezoidal slotted magnetic pole · Surface quality

1 Introduction

Selective laser melting, (SLM) technology is based on laser and powder additive manufacturing technology. The advantage of this technology is the manufacture of complex curved parts. The obvious disadvantage is that the surface roughness of the formed parts is relatively rough [1, 2]. The reason is that this technology forms the parts through a layer-by-layer powder laser melting process. Therefore, it is particularly important to smoothly polish the surface of the formed part. Magnetic abrasive finishing technology is currently more advanced precision finishing technology. It is a finishing method that uses magnetic field force to press magnetically conductive abrasive on the surface of the workpiece for finishing [3]. With high flexibility, it has unique advantages in finishing curved workpieces.

At the same time, magnetic shear thickening finishing/polishing is also an important processing technology that uses magnetic field force to grind workpieces. The paper [4, 5] has a more in-depth study on the finishing mechanism and finishing technology of difficult-to-machine materials such as Ti-6Al-4 V.

In this paper, the magnetic finishing technology is used to apply its inherent advantages of flexible finishing to the finishing of the surface of the curved surface sample of the SLM forming part. At the same time, the finishing experience of the paper [6] is used to analyze the surface quality of the workpiece after finishing. The main research contents include: double-layer parameter optimization printing settings for AlSi10Mg alloy SLM formed curved surface samples; design of spherical 75° trapezoidal grooved permanent

✉ Guixiang Zhang
zhanggx@sdut.edu.cn

1 School of Mechanical Engineering, Shandong University of Technology, Zibo 255000, China

magnet pole finishing tools that can be used for magnetic finishing of curved surface samples; selection of rapid-setting atomization method The prepared spherical Al2O3 magnetic abrasive was used for MAF smoothing orthogonal optimization finishing of SLM shaped curved surface samples, and the best finishing parameters for this type of material were optimized, and the surface roughness, surface morphology and surface of the samples before and after finishing were optimized. The hardness and hydrophobic properties were tested and analyzed, and it was finally found that MAF is suitable for surface finishing and finishing of complex curved parts formed by SLM.

2 Experimental

2.1 Double-layer optimized printing of AlSi10Mg alloy SLM forming curved surface samples

In this paper, AlSi10Mg alloy powder with a particle size range of 23–25 μm provided by Solutions group is used for SLM forming. The SEM and EDS pictures of the powder are shown in Fig. 1, and the powder element composition table is shown in Table 1.

The SLM®125HL selective laser melting forming equipment of German SLM Solutions 3D printing company is used to form AlSi10Mg alloy powder for SLM forming. The forming model refers to the aero engine blade structure for modeling [7–9]. The finished product is shown in Fig. 2e, d. As shown, the forming parameters of the sample are set in layers inside and outside. As shown in Table 2, the outer scanning parameters can increase the surface hardness of the sample while ensuring a low surface roughness, and the internal scanning parameters can improve the compactness of the sample [2].

Figure 2b, c shows the on-site diagram of the finishing sample forming, and the physical diagram of the sample is shown in Fig. 3. Wire EDM is used to separate the sample from the substrate, and then the sample is supported by an ultrasonic cleaner because the magnetic finishing technology

Table 1 AlSi10Mg alloy powder element composition table

Element	Weight %	Atomic %	Net Int
Mg	1.10	1.30	46.25
Al	88.78	89.22	3648.12
Si	10.12	9.48	155.64

selected in this article is high-precision finishing , the original shape of the forming needs to be retained. In order to ensure the accuracy of the later test results, it is selected to retain the residual support sintering point of the sample.

2.2 Detection and analysis of the original morphology of the AlSi10Mg alloy SLM forming surface sample

The surface roughness and surface morphology of the AlSi10Mg alloy SLM curved sample were detected and analyzed by a metallurgical microscope and a white light interferometer. The detection results are shown in Fig. 4. The surface of the unground sample is rough due to the particularity of its forming technology, Ra = 2.12 μm. In addition, due to uneven powder spreading, unbalanced laser density and laser power during forming, unmelted or overmelted AlSi10Mg powder will inevitably exist in the molten pool of the sample. After ultrasonic cleaning, the unmelted powder leaves holes on the surface of the sample, while the overmelted powder will form hemispherical protrusions, and the two combine to form a ravine and vertical microscopic surface morphology.

Vickers hardness tester is used to test the surface hardness of the AlSi10Mg alloy SLM curved surface sample. As shown in Fig. 5, the hardness measurement pressure is $F = 4.9$ N. After pressing it for 15 s, the test diamond appears as shown in Fig. 5c. The original surface hardness of the piece is 126.7HV0.5.

In this paper, a contact angle measuring instrument (OCA15EC) is used to test the deionized water contact angle of the AlSi10Mg alloy SLM surface sample as

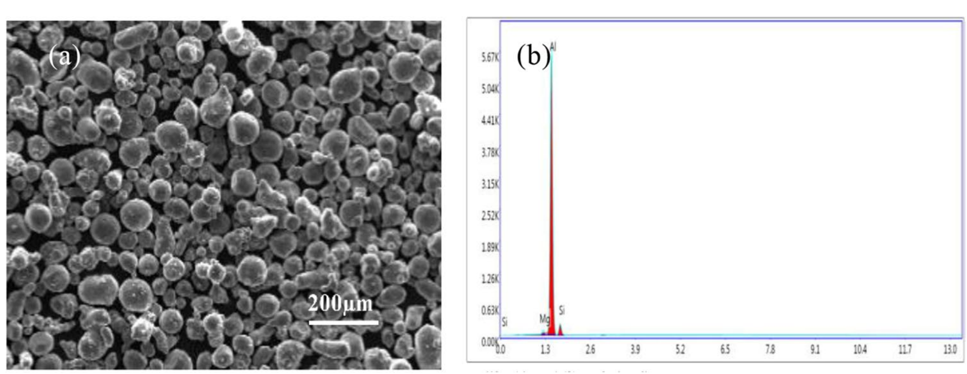

Fig. 1 SEM and EDS images of AlSi10Mg alloy powder. **a** SEM, **b** EDS

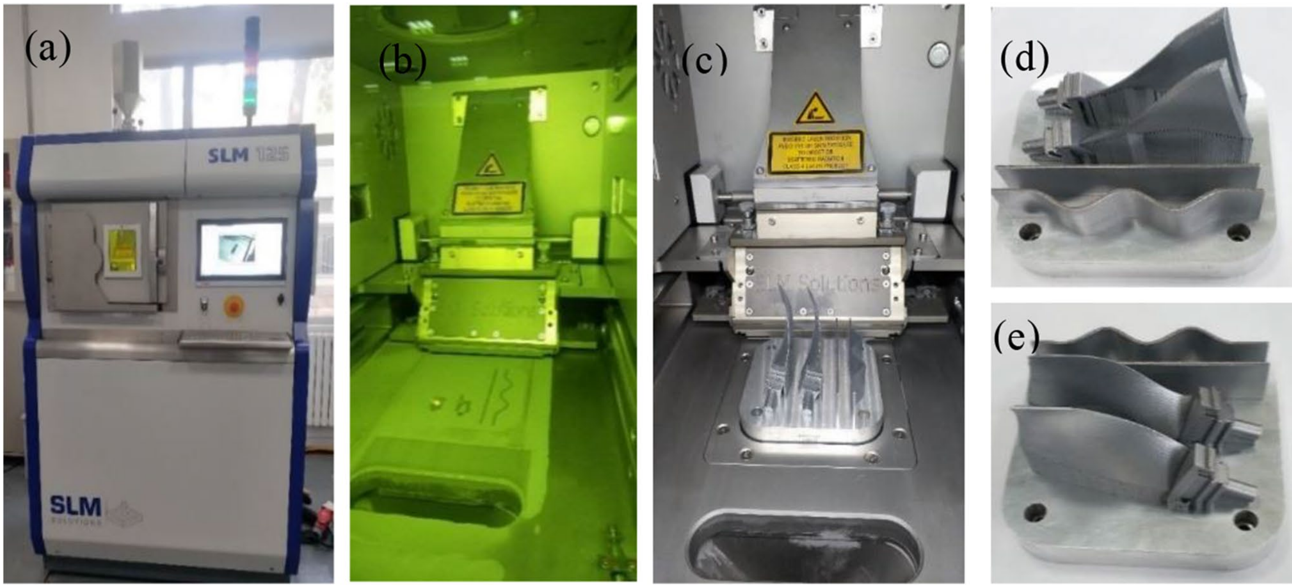

Fig. 2 AlSi10Mg alloy SLM forming surface sample. **a** SLM®125HL forming machine, **b**, **c** forming site diagram, **d**, **e** sample finished product

Table 2 AlSi10Mg alloy SLM forming parameter table

Parameters	Laser power	Scanning speed	thickness of the layer	Scanning interval	Spot size	Scanning way
The outer layer	250 W	2200 mm/s	75 μm	100 μm	80 μm	67°
The inner layer	250 W	1650 mm/s	95 μm	100 μm	80 μm	67°

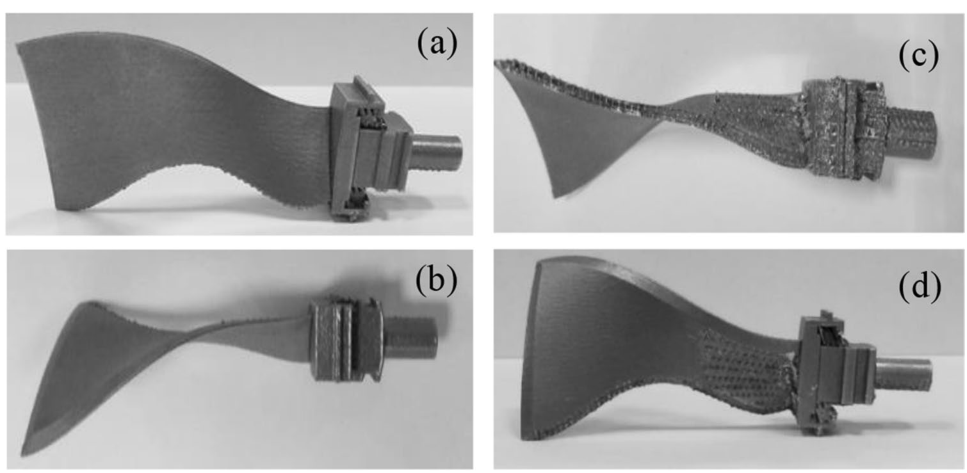

Fig. 3 Physical image of AlSi10Mg alloy SLM forming curved surface sample. **a** Front view, **b** top view, **c** bottom view, **d** rear view

shown in Fig. 6, and the inspection result is shown in Fig. 6c. Therefore, deionized water is divided by a stepped structure and crisscrossed surfaces and cannot exist in the form of large droplets. The contact angle of deionized water is 1.6°, which has strong hydrophilicity.

2.3 Design of permanent magnet finishing device for magnetic finishing of AlSi10Mg alloy SLM shaped surface samples

Magnetic finishing surface parts need to increase the

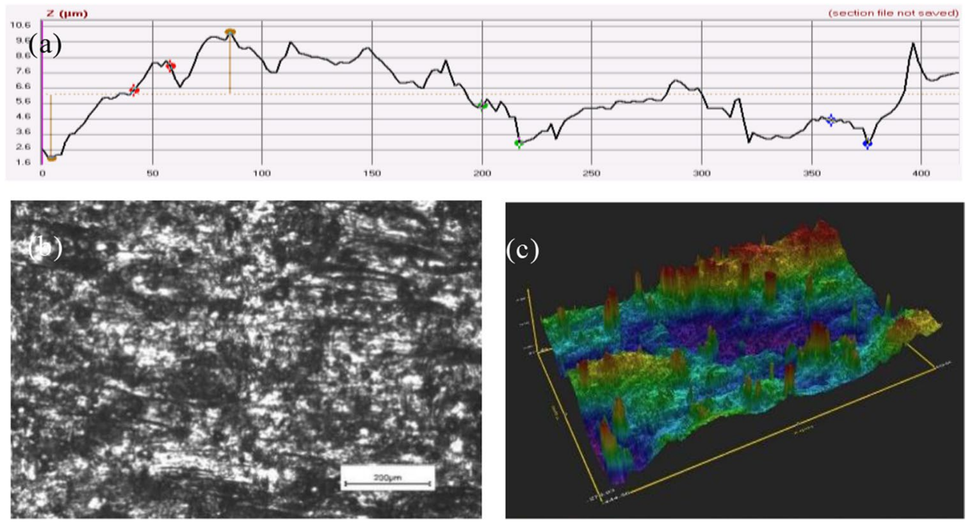

Fig. 4 Surface morphology of AlSi10Mg alloy SLM curved sample. **a** Surface roughness Ra peak-valley diagram, **b** metallographic diagram, **c** three-dimensional topography diagram

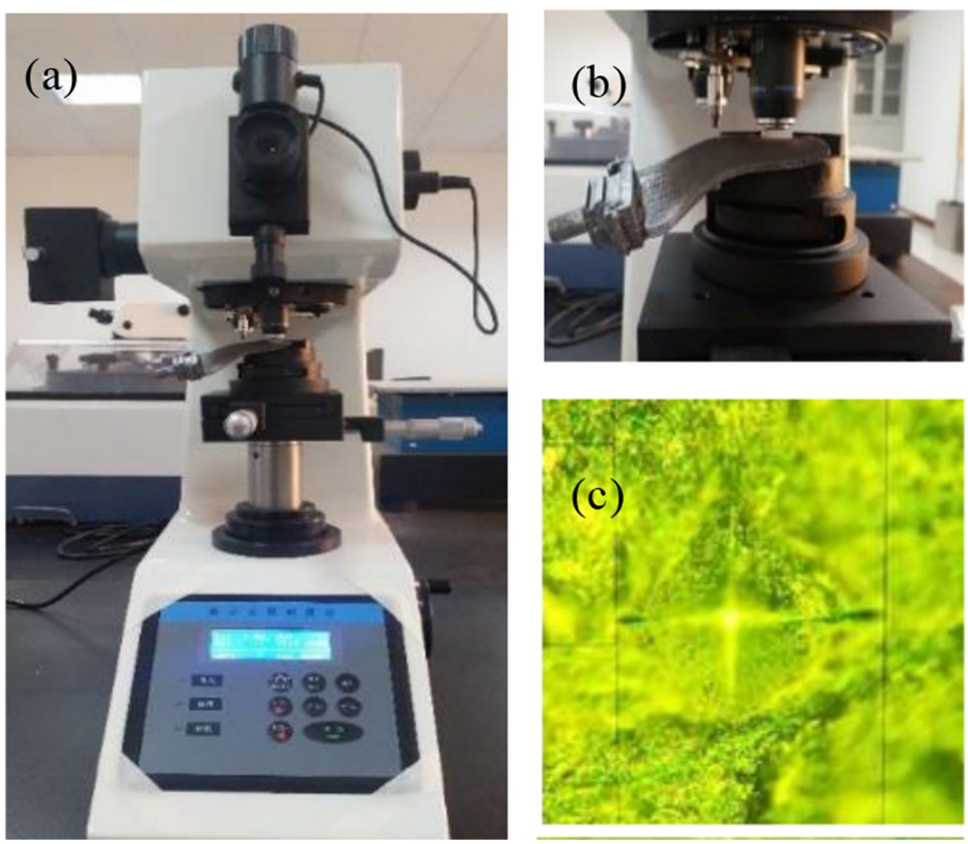

Fig. 5 Vickers hardness test of AlSi10Mg alloy SLM curved sample. **a** Site map, **b** sample inspection, **c** test result

finishing gap to ensure flexible finishing characteristics, so it is necessary to improve the abrasive adsorption performance of the magnetic pole. Through the paper [3], it is found that the magnetic field strength and magnetic field gradient in the magnetic pole processing area are the main factors affecting the finishing effect, so these two factors need to be considered comprehensively in the magnetic pole design. At present, the method of increasing the magnetization of permanent magnetic poles is mainly to slot the finishing surface [10, 11]. Before slotting, the overall size of the finishing magnetic pole needs to be calculated to ensure that the machining gap is 0 ~ 2.5 mm to provide more than 1 T Magnetic field force.

Figure 7 shows a schematic diagram of the magnetic pole finishing of the magnetic finishing ball head. The material for the finishing magnetic pole selected in this study is a rare earth

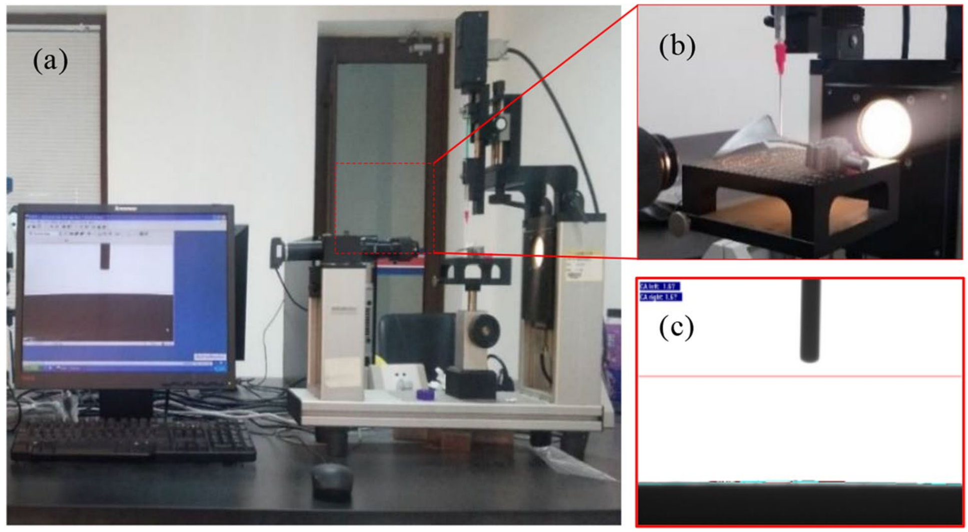

Fig. 6 Hydrophobicity detection of AlSi10Mg alloy SLM curved sample. **a** Site map, **b** sample inspection, **c** test result

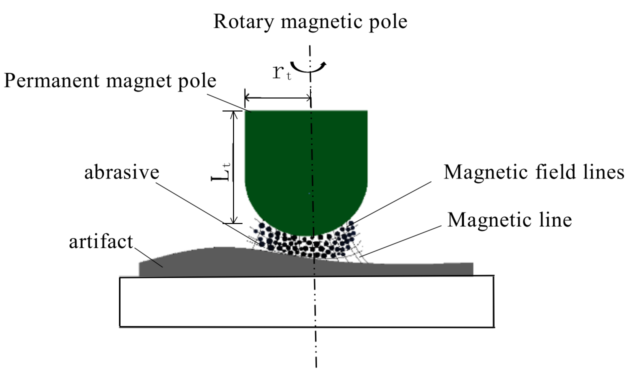

Fig. 7 Schematic diagram of magnetic pole finishing of magnetic finishing ball head

Table 3 Rare earth sintered permanent magnet materials

Remanence B_r(T)	Magnetic energy product $(BH)_{max}$(kJ/m^3)	Coercivity Hc(kA/m)	Density ρ(g/m^3)	Operating temperature Tc(℃)
1.1 ~ 1.2	260 ~ 280	≥ 860	7.45	≤ 80

sintered permanent magnet material, and the parameter performance is shown in Table 3.

$$L_t = fL_g \frac{B_g}{\mu_0}\sqrt{\frac{B_r}{H_C(\mathrm{BH})_{max}}} \quad (1)$$

$$r_t = \sqrt{\mu_0 \sigma S_g \frac{B_g}{3.14\mu_0}\sqrt{\frac{H_c}{B_r(\mathrm{BH})_{max}}}} \quad (2)$$

According to the principle of magnetic flux continuity and the Ampere's loop theorem [12], (1) and (2) are derived, where Lt and rt represent the height and radius of the spherical magnetic pole shown in Fig. 7, according to the rare earths shown in Table 2. The performance parameters of the sintered permanent magnet material are finally calculated as Lt = 13 mm and rt = 12.5 mm.

According to the above dimensions, in order to explore the influence of different slot shapes on the magnetic field strength of the finishing magnetic poles, this paper designs a total of 6 types of slot simulation models with different shapes, as shown in Fig. 8, and the angularity of the various magnetic pole slots is 30° The angle span is decreasing, and 180° is a non-grooving shape. The main parameter setting of the simulation is to use the magnetic field and the steady-state three-dimensional physical field without current for simulation calculation. The excitation source selects the magnetic field applied by the permanent magnet in the axial direction. The values of residual magnetic induction and coercivity are respectively Br = 1 T and Hc = 860 k A/m.

The relationship curve in Fig. 9 shows that the magnetic field strength is inversely proportional to the edge angle of the magnetic pole slot. The smaller the angle, the higher the magnetic field strength. When the angle reaches 30°, the magnetic field strength reaches 1.4 T. But at the same time, it can be found from Fig. 8 that the areas with higher magnetic field strength are mainly concentrated at the sharp points, which are not suitable for the design requirements of magnetic abrasive tools. However, according to the relationship between the magnetic field strength and the slotted edge angle, this experiment designed a 75° trapezoidal slotted magnetic pole with a higher magnetic field strength and a larger distribution area. Including 75° trapezoidal slotted magnetic poles on cylindrical surface and 75°trapezoidal

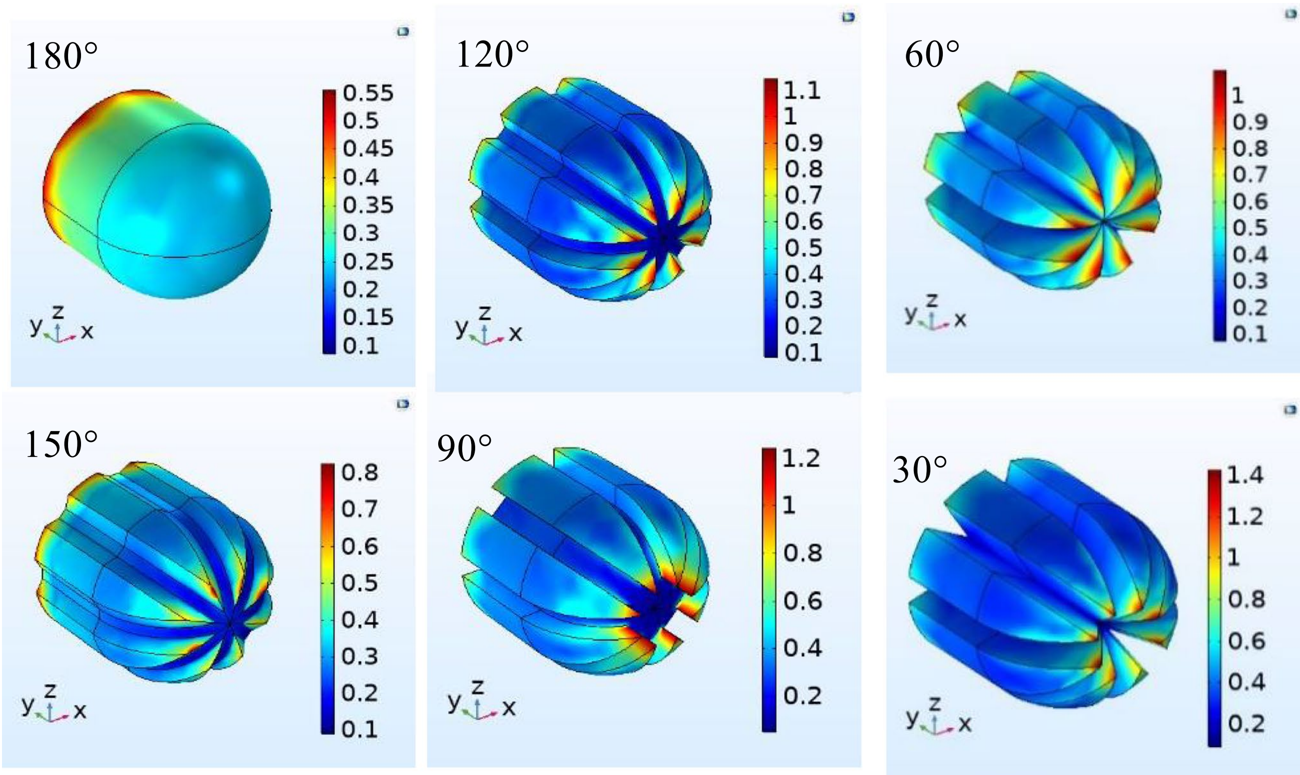

Fig. 8 Cloud map of magnetic field strength simulation results

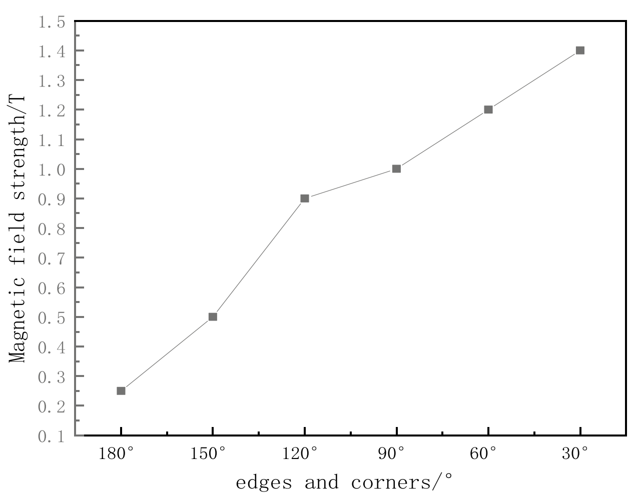

Fig. 9 Relationship curve between magnetic field strength and slotted corner

slotted poles on spherical surface. The ratio of L:H is 2:1. The design dimensions and simulation results are shown in Fig. 10 and Fig. 11.

Through the simulation results shown in Fig. 10a–c and Fig. 11a–c, it can be seen that the magnetic field strength of the slotted surface of the two types of 75° trapezoidal slotted magnetic poles can reach 1.2 T, The area with higher magnetic field strength is larger. At the same time, comparing the simulation results of the slotted magnetic poles with the simulation results of the unslotted raw material in Fig. 10d–f and Fig. 11d–f, it is found that the magnetic field lines in the 75° trapezoidal slotted magnetic pole processing area are more The concentration of the magnetic field gradient is more obvious at the corners of the groove. The reason is that the irregular surface morphology after the groove changes the distribution of the magnetic lines of force, which improves the magnetic field gradient of the finishing area.

Figures 10g and 11g show the actual figure of the ground magnetic pole obtained by compacting the NdFeB rare earth material for high-temperature sintering, magnetizing 1 T longitudinally, and ensuring that the magnetic field strength of the blank surface is not less than 0.95 T according to the design size. Figures 10i and 11i are the effect diagrams of the magnetic poles adsorbing the magnetic abrasive. It can be seen that the magnetic abrasive is evenly distributed on the boss along the edge of the slot.

In order to test the magnetic field strength of the actual magnetic poles, a surface magnetic tester is selected to detect the magnetic field strength of the magnetic pole surface. Figure 12 shows the detection scene. Since the magnetic finishing gap is maximum 2.5 mm, the detection interval is 3 mm. The test results are shown in Fig. 13. The inspection position is the entire slotted surface of the slotted magnetic

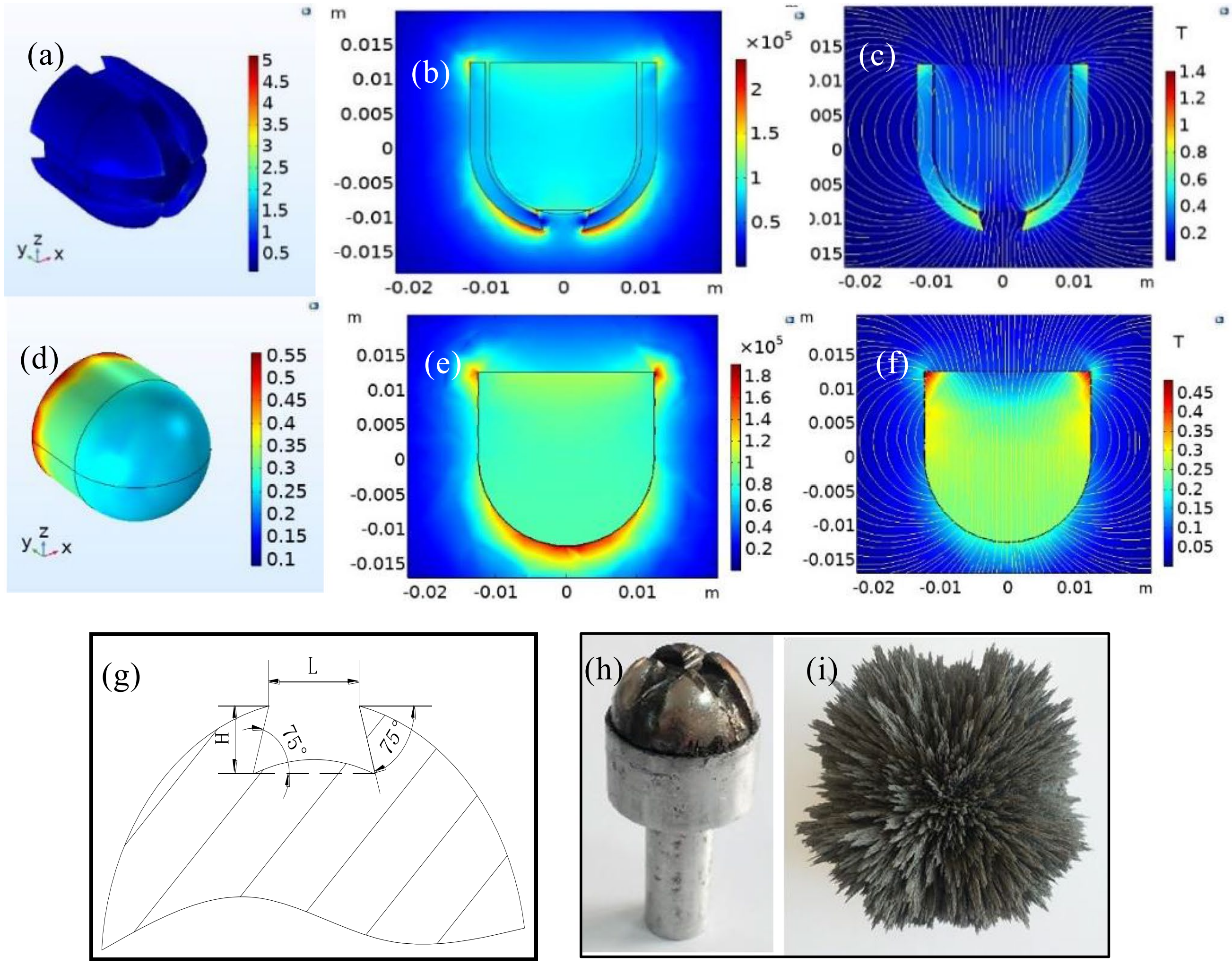

Fig. 10 Various parameters of spherical 75° trapezoidal slotted magnetic pole. **a**, **b**, **d**, **e** Cloud map of magnetic field strength, **c**, **f** cloud map of magnetic field lines, **g** dimensional diagram, **h** physical map, **i** abrasive adsorption effect map

pole. After the inspection table rotates 360°, the probe will detect the magnetic field distribution value of the entire area and generate a distribution map of the inspection result. The zero position of the probe is the position where the magnetic probe touches the surface of the magnetic pole, and the lifting interval is 0.5 mm, and the maximum detection distance is 3 mm. It can be seen that the designed two types of magnetic poles can reach more than 1.1 T within the range of 3 mm, which can meet the requirements of flexible processing of magnetic finishing.

2.4 Finishing test and processing of magnetic abrasive AlSi10Mg alloy SLM forming surface sample

In this paper, the spherical magnetic abrasive prepared by the atomization quick-setting method [3] is used. The abrasive phase is Al2O3 ceramic material, and the size of the abrasive phase is W7. Figure 14 is the scanning electron microscope image of the spherical Al2O3 magnetic abrasive. It can be seen that the iron matrix and the abrasive grain phase has good wettability, and the abrasive grain phase can be firmly adhered to the iron matrix. At the same time, the abrasive sphericity is high, which is conducive to free flow during finishing, thereby ensuring flexible finishing [13, 14].

Multiple papers verified [15–17] that there are three types of finishing states in magnetic finishing, namely, split plow, rolling shear and air running, as shown in Table 3. When the finishing gap is large, the air running phenomenon will appear, as shown in Table 4 (3). When the finishing gap cannot enable the abrasive to be processed flexibly during the finishing process, the tipping plough state shown in Table 4 (1) will appear. Only when the finishing gap is suitable can the rolling shear soft finishing state appear as shown in Table 4 (2).

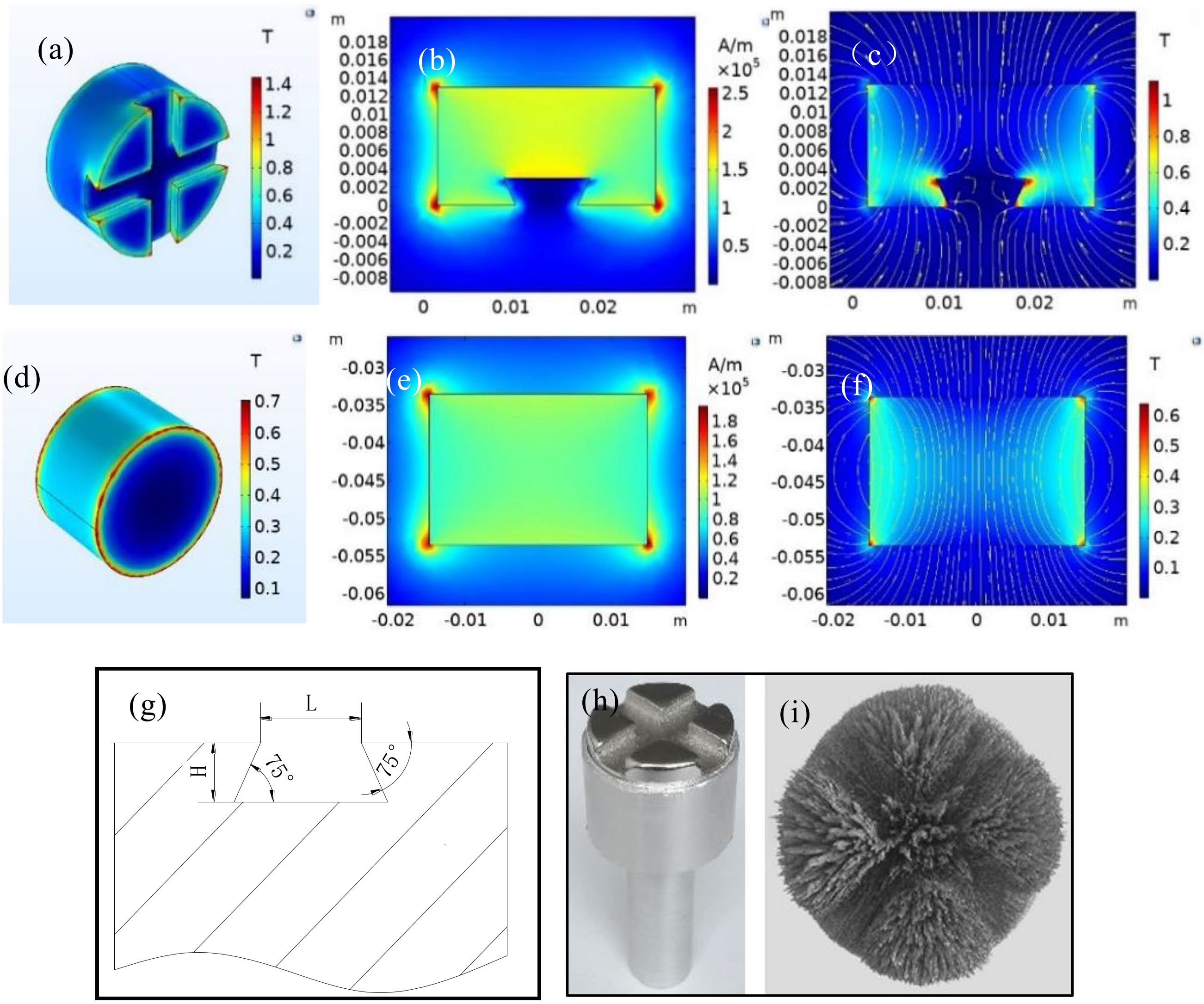

Fig. 11 The parameters of the cylindrical 75° trapezoidal slotted magnetic pole. **a**, **b**, **d**, **e** Cloud map of magnetic field strength, **c**, **f** cloud map of magnetic field lines, **g** dimensional diagram, **h** physical map, **i** abrasive adsorption effect map

The sample to be polished in this experiment should not only select a suitable finishing gap, but also consider the surface characteristics of the sample. Therefore, it is designed to use cylindrical 75° trapezoidal slotted magnetic poles with higher magnetic field strength to adsorb magnetic abrasives for the initial finishing of the workpiece, and set a higher finishing gap to avoid the interference of the surface features of the sample, so as to remove the bulk of the surface of the sample. The crusted part left by sintering completely AlSi10Mg alloy. Then, the spherical 75° slotted magnetic pole is used to absorb the magnetic abrasive, and the innate advantage that the magnetic pole does not interfere with the curved sample is used to carry out the perfect lamination and finishing of the sample. The schematic diagram of the finishing is shown in Figs. 15 and 16.

At the same time, this experiment uses a 3-level 4-factor orthogonal test table to carry out 27 sets of finishing experiments. Each group includes two parts: initial finishing and re-finishing, and empirically optimized finishing for important finishing parameters such as Spindle speed, Feed rate, gap and Abrasive consumption. Figure 17 is a diagram of the finishing site, and Table 5 is a table of finishing parameters. In the magnetic finishing process, due to the large size of the magnetic pole and the irregular shape of the workpiece, the numerical control points of the finishing track of the machine tool can be processed by the computer-aided software Mastercam. The centering of the tool can be set using a universal edge finder, as shown in Fig. 17e. The X1, X2, Y1, Y2, and Z0 coordinate positions of the workpiece are detected by the probe of the universal edge finder to realize the establishment of the workpiece coordinate system.

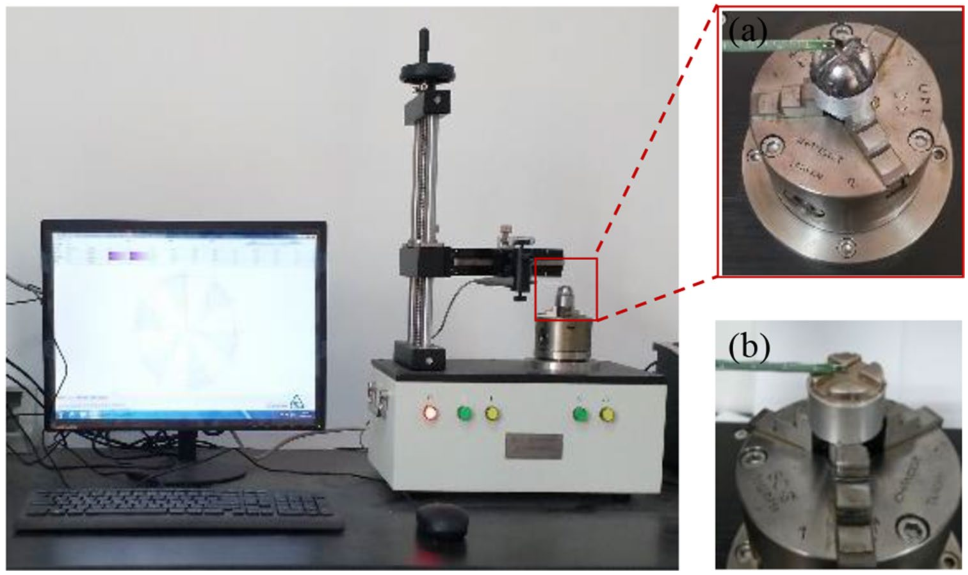

Fig. 12 75° Trapezoidal slotted permanent magnet pole magnetic field strength detection. **a** Spherical magnetic pole, **b** Cylindrical magnetic pole

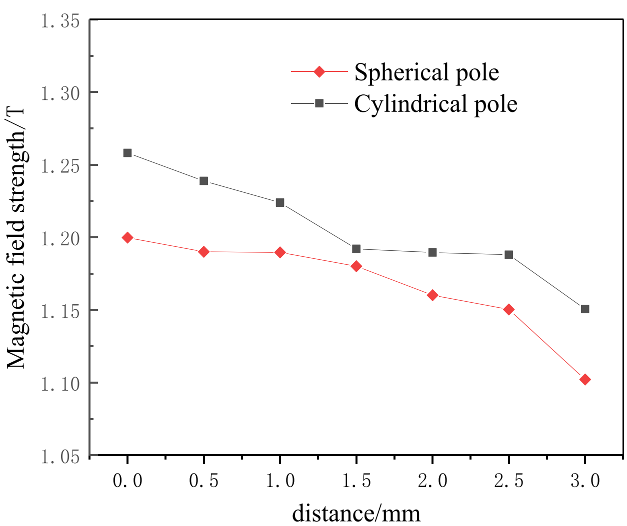

Fig. 13 The magnetic field strength of a 75° trapezoidal slotted pole surface varies with distance

Because the tool diameter is large, the initial position of the finishing tool can be offset by one radius from the tool in the positive direction of the X axis as the starting position.

Table 6 is a summary table of the finishing effect, taking into account the interaction between various factors, the results of the three sets of interaction tests between ($A \times B$), ($A \times C$) and ($B \times C$). By analyzing the orthogonal test table, the best combination of finishing parameters can be calculated, which are s1, f3, h2 and g2, and the corresponding finishing parameter values are 1800 r/min, 5 mm/min, 2 mm and 7 g. The range distribution of each factor is $A > B > D > C$. It can be seen from Fig. 18 that the influence ratio of the amount of abrasive is greater than the influence ratio of the finishing gap. For the magnetic finishing of the AlSi10Mg alloy SLM surface, the finishing state is affected. The primary factor is the amount of abrasive filling, too much abrasive filling will affect the flexibility characteristics of magnetic finishing.

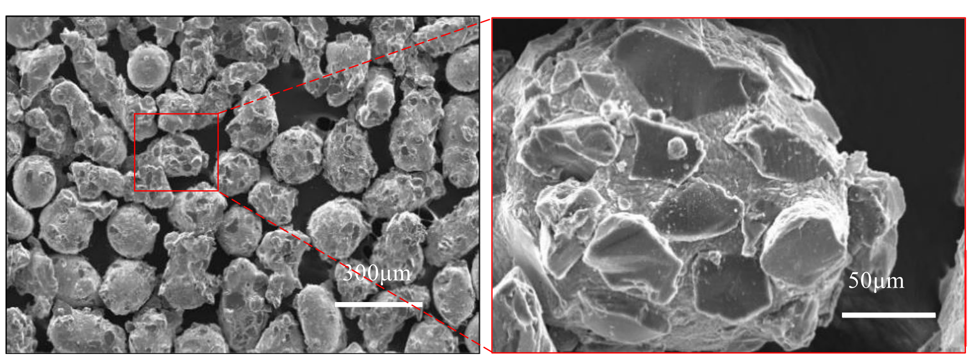

Fig. 14 SEM image of spherical Al2O3 magnetic abrasive

Table 4 Abrasive movement state classification table

Number	Abrasive finishing movement diagram	Classification
(1)	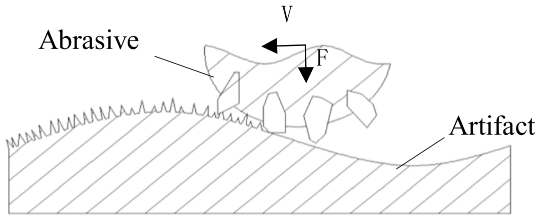	Slash plough
(2)	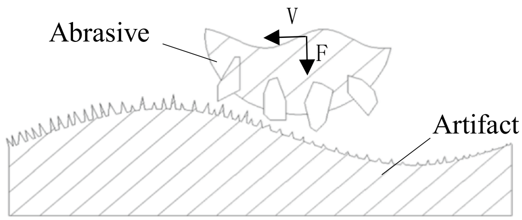	Rolling cut
(3)	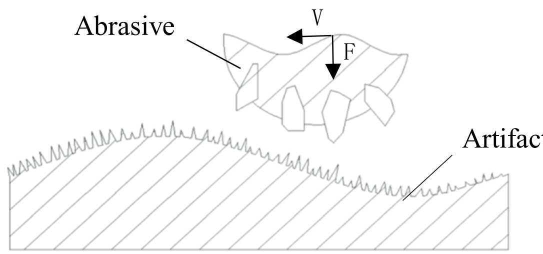	Empty run

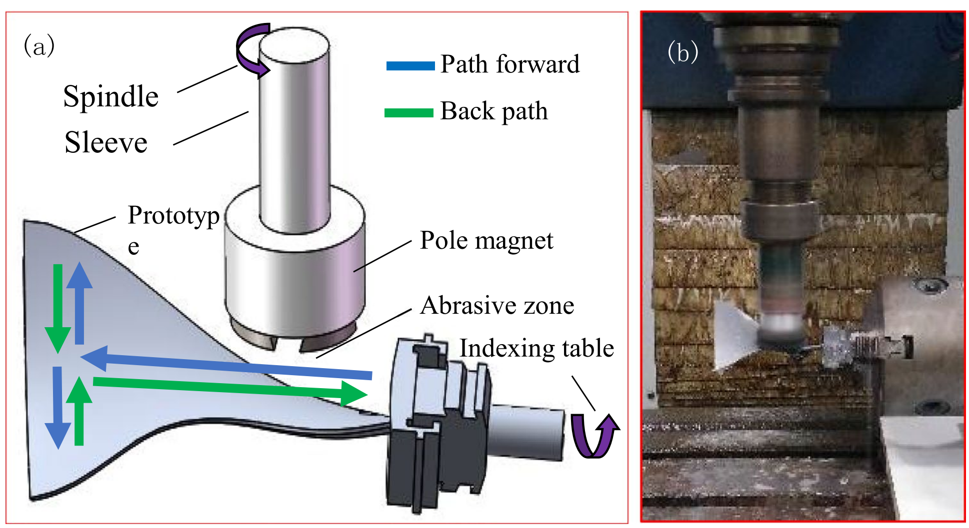

Fig. 15 Schematic diagram of the initial finishing of a sample using a cylindrical 75° trapezoidal slotted magnetic pole. **a** Schematic diagram of finishing path, **b** finishing site diagram

3 Results

3.1 Surface roughness detection and analysis

The best finishing parameters calculated by the orthogonal test method are used to magnetically grind the AlSi10Mg alloy SLM shaped curved surface sample. During the finishing process, a white light interferometer is used to detect the surface roughness of the sample, and multiple areas are tested each time, and the average value is taken. At the same time, an electronic balance is used to count the material removal of the sample. Finally, the change curve shown in Fig. 19 is drawn. In the Fig, 0–6 min is the initial finishing roughness change curve using cylindrical 75° trapezoidal slotted magnetic poles, and 6–16 min is the

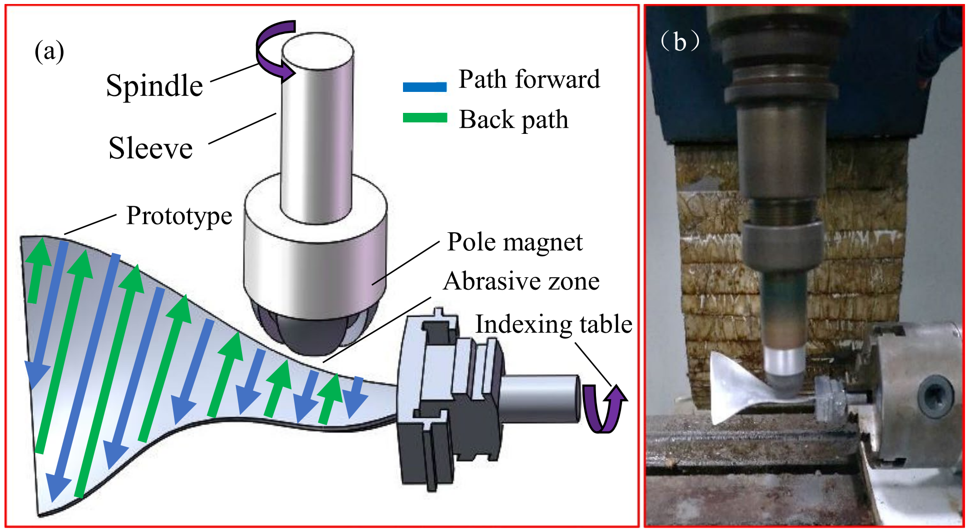

Fig. 16 Schematic diagram of re-finishing the sample using spherical 75° trapezoidal slotted magnetic poles. **a** Schematic diagram of finishing path, **b** finishing site diagram

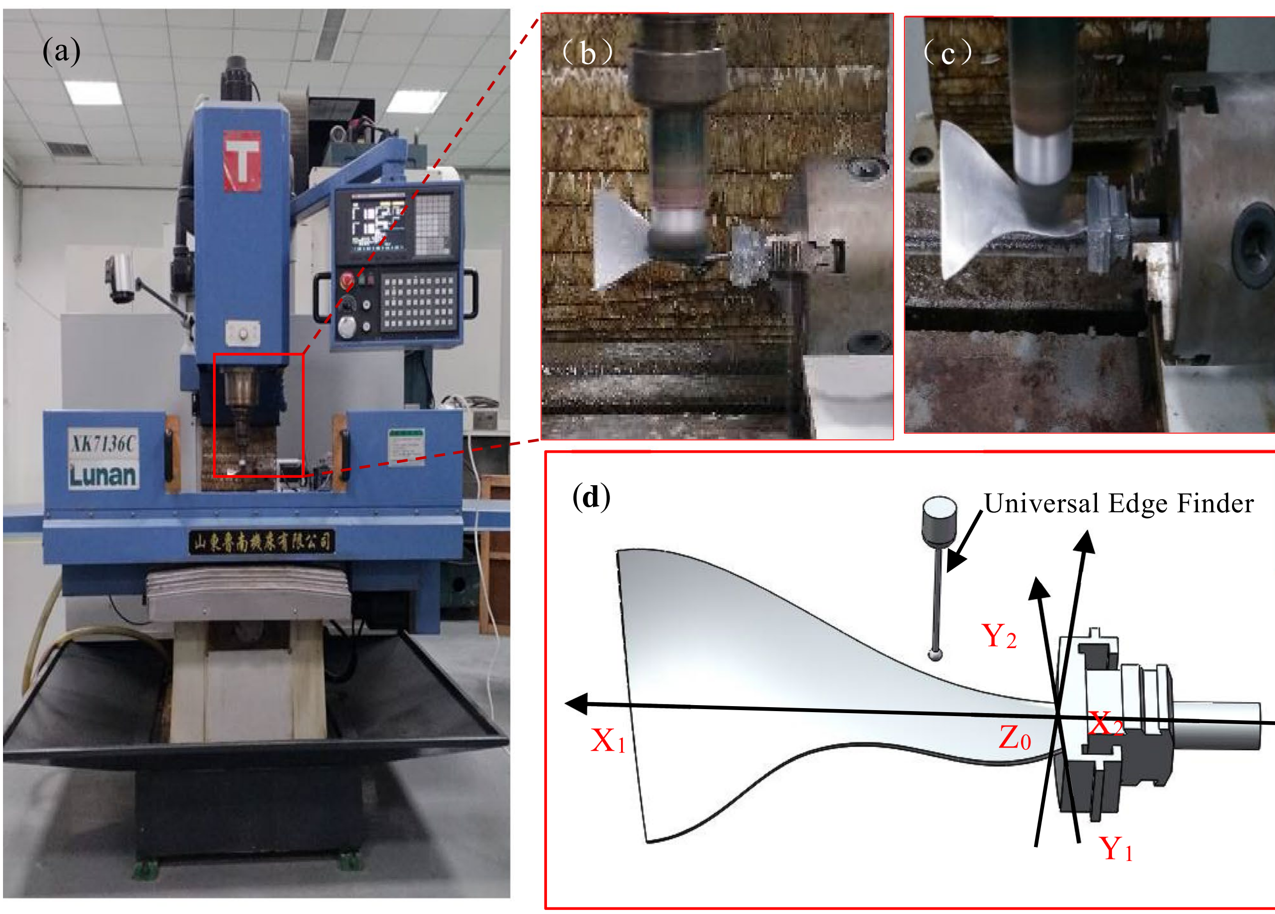

Fig. 17 Magnetic finishing scene of AlSi10Mg alloy SLM forming surface sample. **a** Site map, **b** initial finishing, **c** re-grind, **d** schematic diagram of knife setting

Table 5 3 Distribution table of 3-level 4 factor orthogonal test

Level	Spindle speed	Feed rate	Gap	Abrasive consumption
	A(s)	*B*(f)	*C*(h)	*D*(g)
1	1800 r/min	12 mm/min	2.5 mm	10 g
2	1500 r/min	8 mm/min	2 mm	7 g
3	1200 r/min	5 mm/min	1.5 mm	3.5 g

roughness change curve using spherical 75° trapezoidal slotted magnetic poles for re-finishing.

The detection area selected in this article is any area of the sample with 1cm^2. When the feed rate of the optimal finishing parameter is determined to be 5 mm/min, then according to the rough finishing path generated by the Mastercam auxiliary software, the actual effective finishing track length can be calculated as 170 mm, the calculated rough finishing time is 34 min. Through the integral calculation of the surface area of one side of the curved sample, it can be known that the finishing area of the sample is 2216.92 mm^2, so the single rough finishing time corresponding to the sample area with the detection unit of 1 cm^2 is 2 min. In the same way,

Table 6 Summary table of magnetic finishing effects of AlSi10Mg alloy SLM formed curved surface samples

Orthogonal interactive test table								
Number	*A*	*B*	*A*×*B*	*C*	*A*×*C*	*B*×*C*	*D*	Ra/μm
1	s1	f1	s1 f1	h1	s1 h1	f1 h1	g1	0.302
2	s1	f1	s1 f1	h2	s2 h2	f2 h2	g2	0.312
3	s1	f1	s1 f1	h3	s3 h3	f3 h3	g3	0.355
4	s1	f2	s2 f2	h1	s1 h1	f2 h3	g3	0.368
5	s1	f2	s2 f2	h2	s2 h2	f3 h1	g1	0.362
6	s1	f2	s2 f2	h3	s3 h3	f1 h2	g2	0.336
7	s1	f3	s3 f3	h1	s1 h1	f3 h2	g2	0.282
8	s1	f3	s3 f3	h2	s2 h2	f1 h3	g3	0.291
9	s1	f3	s3 f3	h3	s3 h3	f2 h1	g1	0.282
10	s2	f1	s2 f3	h1	s2 h3	f1 h1	g2	0.459
11	s2	f1	s2 f3	h2	s3 h1	f2 h2	g3	0.428
12	s2	f1	s2 f3	h3	s1 h2	f3 h3	g1	0.413
13	s2	f2	s3 f1	h1	s2 h3	f2 h3	g1	0.411
14	s2	f2	s3 f1	h2	s3 h1	f3 h1	g2	0.396
15	s2	f2	s3 f1	h3	s1 h2	f1 h2	g3	0.403
16	s2	f3	s1 f2	h1	s2 h3	f3 h2	g3	0.413
17	s2	f3	s1 f2	h2	s3 h1	f1 h3	g1	0.408
18	s2	f3	s1 f2	h3	s1 h2	f2 h1	g2	0.399
19	s3	f1	s3 f2	h1	s3 h2	f1 h1	g3	0.486
20	s3	f1	s3 f2	h2	s1 h3	f2 h2	g1	0.452
21	s3	f1	s3 f2	h3	s2 h1	f3 h3	g2	0.467
22	s3	f2	s1 f3	h1	s3 h2	f2 h3	g2	0.428
23	s3	f2	s1 f3	h2	s1 h3	f3 h1	g3	0.426
24	s3	f2	s1 f3	h3	s2 h1	f1 h2	g1	0.482
25	s3	f3	s2 f1	h1	s3 h2	f3 h2	g1	0.472
26	s3	f3	s2 f1	h2	s1 h3	f1 h3	g2	0.433
27	s3	f3	s2 f1	h3	s2 h1	f2 h1	g3	0.466
I	2.887	3.674	3.525 3.55	3.618	3.475 3.596	3.600 3.578	3.584	
II	3.73	3.612	3.737 3.691	3.508	3.663 3.566	3.546 3.577	3.509	
III	4.112	3.443	3.467 3.488	3.603	3.591 3.567	3.583 3.574	3.636	
Ki	3	3	3	3	3	3	3	
I/k1	0.962	1.224	1.175 1.183	1.206	1.158 1.198	1.200 1.193	1.194	
IIk2	1.243	1.204	1.245 1.230	1.169	1.221 1.188	1.182 1.192	1.169	
III/k3	1.370	1.147	1.155 1.162	1.201	1.197 1.189	1.194 1.191	1.212	
极差	0.281	0.077	0.090 0.068	0.037	0.063 0.010	0.018 0.002	0.043	

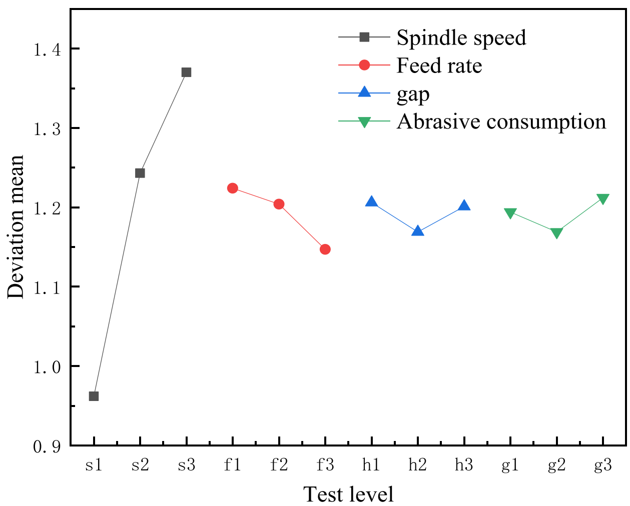

Fig. 18 The relationship between the level of various factors and the surface roughness of the sample

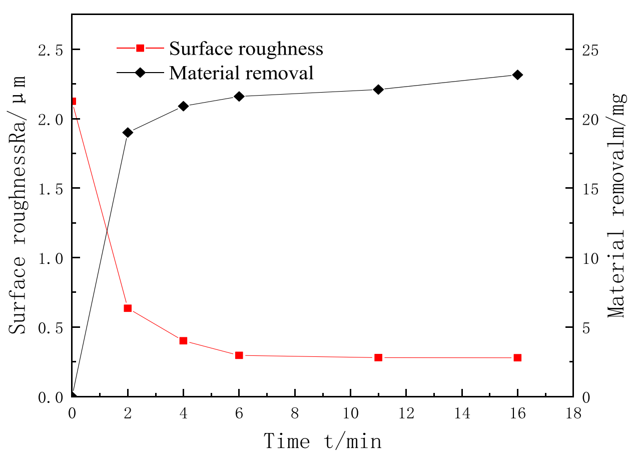

Fig. 19 The surface roughness of the sample and the material removal curve with time

the length of the finishing track for fine finishing is 551 mm, so the single fine finishing time corresponding to the sample area with the detection unit of 1 cm^2 is 5 min.

It can be seen from Fig. 19 that the surface roughness of the sample surface decreases with the increase of processing time during the finishing process. Within 0–6 min of finishing, the sharp point effect is obvious, from the original roughness Ra = 2.12 μm to Ra = 0.296 μm, reflecting the adaptive advantage of magnetic finishing in surface finishing. As the processing time increases, the surface roughness appears to slowly decrease. When the cumulative time reaches 11 min, the surface roughness decreases to Ra = 0.280 μm. When the finishing time reaches 16 min, the surface roughness reaches the minimum Ra = 0.279 μm status.

After finishing, the surface of the sample is polished and polished by the magnetic abrasive to polish and flatten the vertical and horizontal micro morphology of the surface of the sample. As shown in Fig. 20b, c, the surface morphology has been greatly improved. Figure 21 shows the changes in the surface effect of the sample before and after the magnetic finishing. It is finally proved that using the 75° trapezoidal slotted magnetic pole to adsorb the Al2O3 spherical abrasive to the AlSi10Mg alloy SLM shaped curved surface can achieve a better finishing effect. This method can quickly reduce the surface roughness of the sample, and improve the surface morphology of the sample.

3.2 Analysis of Vickers hardness test of finishing surface

In order to detect the influence of magnetic finishing technology on the surface hardness of AlSi10Mg alloy SLM forming curved surface samples, the FM-800 microhardness tester was used to detect the surface hardness changes of the samples during the finishing process, as shown in Fig. 22. It can be seen that during the finishing process, the surface hardness of the sample always fluctuates with 126.7HV0.5 as the baseline, and its floating range is ± 5HV0.5, which is within a reasonable detection error. It can be seen that while the magnetic finishing technology improves the surface roughness of the AlSi10Mg alloy SLM forming curved surface sample, it does not change the surface hardness of the sample.

3.3 Surface hydrophobicity detection and analysis

In this paper, a contact angle measuring instrument (OCA15EC) is used to measure the contact angle of the sample with deionized water before and after finishing to determine the changes in the hydrophilic and hydrophobicity of the sample surface before and after finishing [18], as shown in Fig. 23, the results found that after finishing AlSi10Mg alloy SLM forming surface has obvious changes in affinity. The superhydrophilic surface (θ = 1.6°) before finishing is shown in Fig. 23a, c, and it becomes hydrophilic surface (θ = 61.3°) after finishing.), as shown in Fig. 23b, d.

Because the surface of the sample is polished to obtain a better surface quality, deionized water can adhere to the surface of the sample in the form of a larger droplet, and the surface performance of the sample changes from a superhydrophilic surface to a hydrophilic surface. It can be seen that the surface roughness of the AlSi10Mg alloy SLM shaped surface sample is improved after magnetic finishing, and the hydrophobicity of the surface has also changed from a super-hydrophilic surface to a hydrophilic surface.

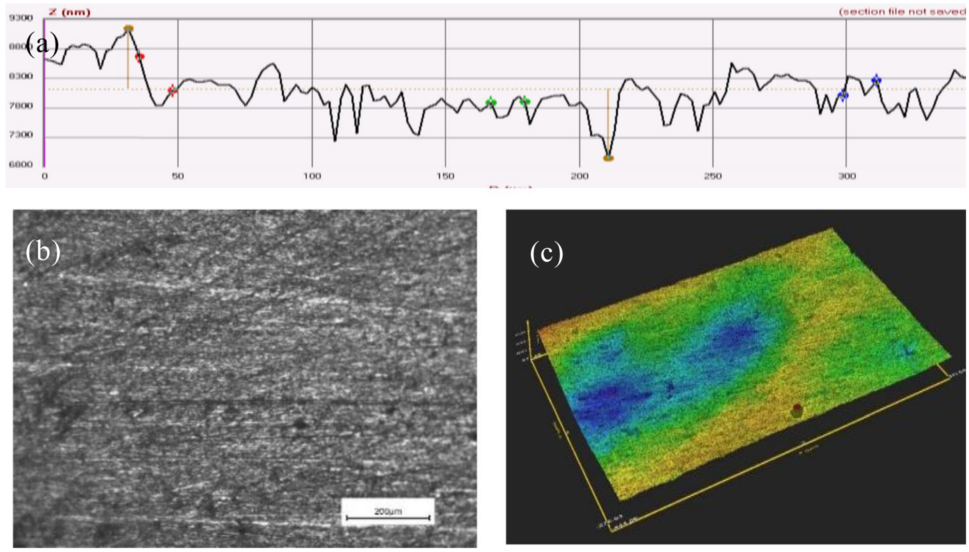

Fig. 20 Surface topography of the sample after finishing. **a** Surface roughness Ra peak-valley diagram, **b** metallographic diagram, **c** three-dimensional topography diagram

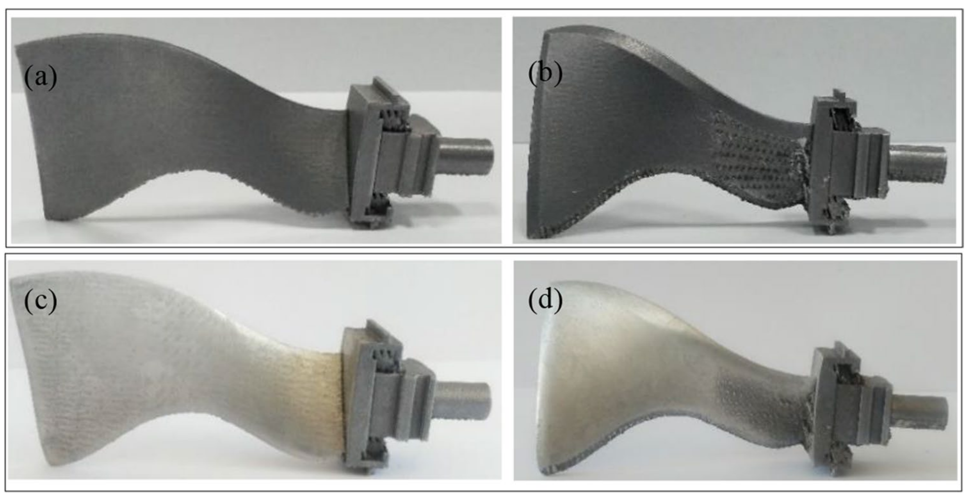

Fig. 21 Comparison of the effect of sample before and after finishing. **a**, **b** Before finishing, **c**, **d** after finishing

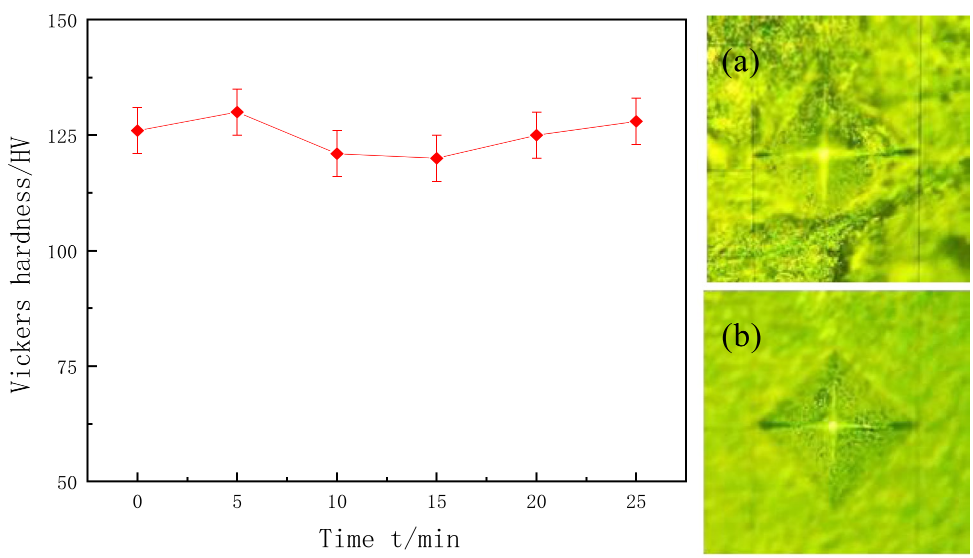

Fig. 22 Variation curve of Vickers hardness of finishing sample with finishing time. **a** Before finishing, **b** after finishing

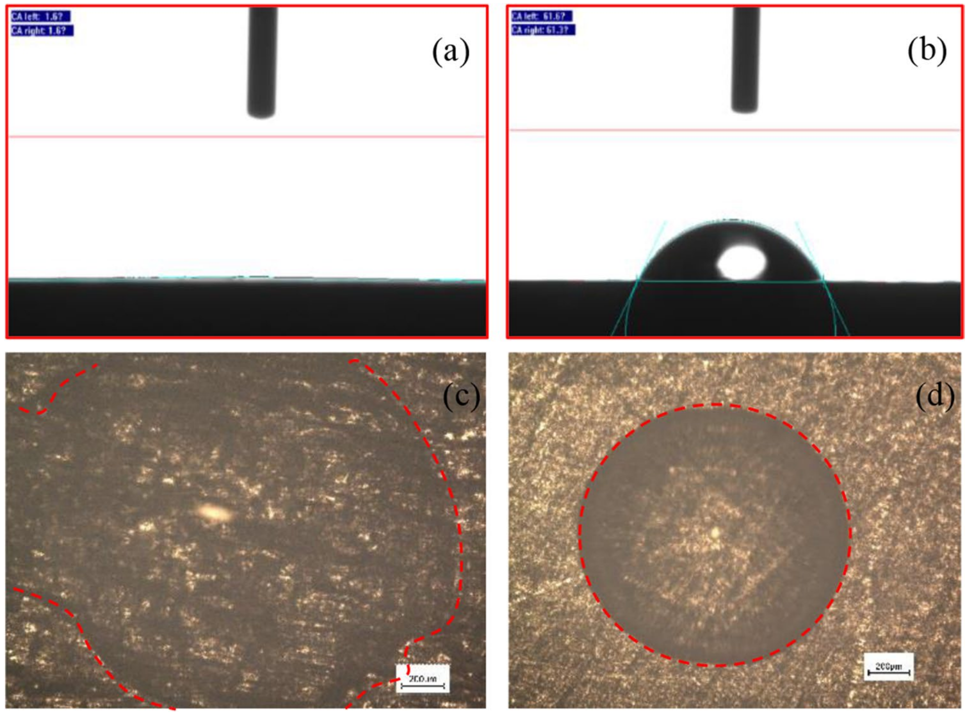

Fig. 23 Comparison of hydrophilicity and hydrophobicity of sample before and after finishing. **a**, **c** Before finishing, **b**, **d** after finishing

4 Conclusion

1. Through simulation analysis and physical inspection, it is found that the 75° trapezoidal slotted permanent magnet finishing tool can be suitable for the finishing needs of AlSi10Mg alloy SLM shaped curved surface samples, and the surface magnetic field strength can reach 1.1 T or more within 3 mm of the finishing area.
2. According to the orthogonal test table, the AlSi10Mg alloy SLM shaped curved surface samples were optimized and ground using different process routes. Finally, it was found that the surface roughness can be obtained when the finishing parameters are 1800 r/min, 5 mm/min, 2 mm and 7 g. The degree of Ra = 0.279 μm in the best state, and the surface morphology of the sample has been greatly improved.
3. While the magnetic finishing technology improves the surface roughness of the AlSi10Mg alloy SLM forming surface sample, it does not change the surface hardness of the sample. But it can significantly improve the hydrophobicity of the sample surface.

Acknowledgements This work is supported by the National Natural Science Foundation of China (No. 51675316).

Author contributions YC contributed the experiment and result analysis of the whole paper, and completed the manuscript writing, comment writing and editing. GZ contributed to the writing of the review, editing, and funding acquisition. TC, PZ, JD, NL and HC contributed to the review and editing with the order provided.

Funding This work is supported by the National Natural Science Foundation of China (No. 51675316).

Data availability The data and materials set supporting the results of this article are included in the ending of the text.

Declarations

Conflict of interest The authors declare that they have no competing interests.

Ethical approval Not applicable.

Consent to participate The manuscript has been read and approved by all named authors.

Consent to publish All the authors listed in the manuscript have approved the manuscript will be considered for publication in The International Journal of Advanced Manufacturing Technology.

References

1. Teng X, Zhang G, Zhao Y, Cui Y, Li L, Jiang L (2019) Study on magnetic abrasive finishing of AlSi10Mg alloy prepared by selective laser melting. Int J Adv Manuf Technol 105:2513–2521. https://doi.org/10.1007/s00170-019-04485-5
2. Teng X, Zhang G, Liang J, Li H, Liu Q, Cui Y, Cui T, Jiang L (2019) Parameter optimization and microhardness experiment of AlSi10Mg alloy prepared by selective laser melting. Mater Res Express 6:086592. https://doi.org/10.1088/2053-1591/ab18d0
3. Zhang G (2012) Study on preparation of magnetic abrasives by gas atomization with rapid solidification and their finishing

performance. University of Aeronautics and Astronautics. http://cdmd.cnki.com.cn/Article/CDMD-10287-1014060820.htm. Accessed 1 June 2012
4. Fan Z, Tian Y, Zhou Q, Shi C (2020) Enhanced magnetic abrasive finishing of Ti–6Al–4V using shear thickening fluids additives. Precis Eng 64:300–306. https://doi.org/10.1016/j.precisioneng2020.05.001
5. Tian Y, Shi C, Fan Z, Zhou Q (2020) Experimental investigations on magnetic abrasive finishing of Ti-6Al-4V using a multiple pole-tip finishing tool. Int J Adv Manuf Technol. https://doi.org/10.1007/s00170-019-04871-z
6. Fan Z, Tian Y, Zhou Q, Shi C (2020) A magnetic shear thickening media in magnetic field–assisted surface finishing. Proc Inst Mech Eng, Part B: J Eng Manuf 234:1069–1072. https://doi.org/10.1177/0954405419896119
7. Geoff H. The aviation industry is moving towards a sustainable future. China Civil Aviation News, 2020-12-11(004). http://www.cannews.com.cn/2020/12/11/99316717.html. Accessed 11 Dec 2020
8. Бойков БВ (1955) Aero engine (trans: Liu S, Zhou T). National Defense Industry Press, Beijing
9. Максай АВ, Полянский НИ (1956) Principles of Aero Engines (trans: Tian W and others). National Defense Industry Press, Beijing
10. Wu J, Zou Y, Sugiyama H (2015) Study on finish characteristics of magnetic abrasive finishing process using low-frequency alternating magnetic field. Int J Adv Manuf Technol 85:585–594. https://doi.org/10.1007/s00170-015-7962-9
11. Zhang P, Zhang G, Liang W (2018) Re-search on magnetic abrasive finishing processes of aluminum magnesium alloy permanent magnet poles. China Mech Eng 29(11):1324–1328
12. Jain VK, Prashant K, Behera PK, Jayswal SC (2001) Effect of working gap and circumferential speed on the performance of magnetic abrasive finishing process. Wear 250:384–390
13. Zhang G, Zhao Y, Zhao D, Yin F, Zhao Z (2011) Preparation of white alumina spherical composite magnetic abrasive by gas atomization and rapid solidification. Scr Mater 65(5):416–419
14. Zhang G, Zhao Y, Zhao D, Zuo D, Yin F (2013) New iron-BASED SiC spherical composite magnetic abrasive for magnetic abrasive finishing. Chin J Mech Eng 26(02):377–383
15. Chen C (2016) Research on the mechanism and basic experiment of magnetic finishing of nickel-based superalloys. Shandong University of Technology. http://cdmd.cnki.com.cn/Article/CDMD-10433-1016231028.htm. Accessed 20 April 2016
16. Zhang P (2018) Fundamental experimental research on magnetic finishing of aluminum-magnesium alloy. Shandong University of Technology. http://cdmd.cnki.com.cn/Article/CDMD-10433 1018139439.htm. Accessed 10 April 2018
17. Zhang P (2012) Experimental research on permanent magnetic field spherical magnetic abrasive magnetic finishing. Shandong University of Technology. http://cdmd.cnki.com.cn/Article/CDMD-10433-1015534946.htm. Accessed 20 Feb 2012
18. Premkumar JR, Khoo SB (2005) Electrochemically generated super-hydrophilic surfaces. Chem Commun 36(15):640–642